Environmental Science & Technology

Article

pubs.acs.org/est

Rapid Mobilization of Noncrystalline U(IV) Coupled with FeS Oxidation

Yuqiang Bi,[†] Malgorzata Stylo,[‡] Rizlan Bernier-Latmani,[‡] and Kim F. Hayes*[,†]

[†]Civil and Environmental Engineering, University of Michigan, Ann Arbor, Michigan 48109, United States

[‡]Environmental Microbiology Laboratory, Ecole Polytechnique Fédérale de Lausanne, CH-1015 Lausanne, Switzerland

Supporting Information

ABSTRACT: The reactivity of disordered, noncrystalline U(IV) species remains poorly characterized despite their prevalence in biostimulated sediments. Because of the lack of crystalline structure, noncrystalline U(IV) may be susceptible to oxidative mobilization under oxic conditions. The present study investigated the mechanism and rate of oxidation of biogenic noncrystalline U(IV) by dissolved oxygen (DO) in the presence of mackinawite (FeS). Previously recognized as an effective reductant and oxygen scavenger, nanoparticulate FeS was evaluated for its role in influencing U release in a flow-through system as a function of pH and carbonate concentration. The results demonstrated that noncrystalline U(IV) was more susceptible to oxidation than uraninite (UO_2) in the presence of dissolved carbonate. A rapid release of U occurred immediately after FeS addition without exhibiting a temporary inhibition stage, as was observed during the oxidation of UO_2, although FeS still kept DO levels low. X-ray photoelectron spectroscopy (XPS) characterized a transient surface Fe(III) species during the initial FeS oxidation, which was likely responsible for oxidizing noncrystalline U(IV) in addition to oxygen. In the absence of carbonate, however, the release of dissolved U was significantly hindered as a result of U adsorption by FeS oxidation products. This study illustrates the strong interactions between iron sulfide and U(IV) species during redox transformation and implies the lability of biogenic noncrystalline U(IV) species in the subsurface environment when subjected to redox cycling events.

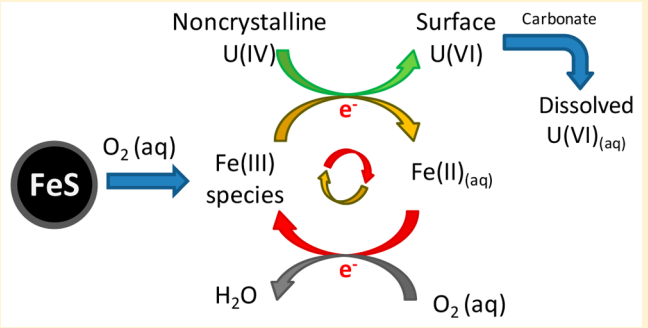

INTRODUCTION

Decades after the end of active uranium mining, milling, and processing, uranium contamination in the subsurface environment remains problematic and represents a public health threat across the United States. Given that U mobility is strongly related to its oxidation state,[1] the transformation of soluble and mobile U(VI) to reduced and relatively immobile U(IV) is a desirable strategy for effective in situ U remediation.[2−4] Until recently, the sparingly soluble uraninite mineral ($UO_{2(s)}$) was considered to be the sole product of U(VI) reduction.[1,5,6] An increasing number of studies have revealed the existence of disordered, noncrystalline U(IV) species, which are characterized by the absence of U−U pair backscattering at 3.8 Å in X-ray absorption spectroscopy (XAS) data.[7−9] Both laboratory[8−10] and field[11−14] research suggest the prevalence of this U(IV) species as a result of association of U(IV) with EPS from biofilms after active U bioremediation. Unfortunately, limited thermodynamic and structural information on noncrystalline U(IV) is available,[7,15] rendering the current geochemical models insufficient for evaluating U stability and optimal conditions for cleanup efforts.

Because of the lack of crystalline structure, noncrystalline U(IV) is likely more labile and susceptible to reoxidation and complexation than UO_2 in subsurface environments. Only a few studies, however, have examined the reactivity of biogenic noncrystalline U(IV) in laboratory systems.[16,17] Alessi et al.[16] showed that the noncrystalline U(IV) fraction can be selectively extracted from a U(IV)−U(VI) mixture by an anoxic 1 M bicarbonate solution. Cerrato et al.[17] further demonstrated that the U(IV) species can be readily oxidized by dissolved oxygen (DO) and persulfate. In a heterogeneous subsurface environment, various complexing ligands (i.e., carbonate) and oxidants (i.e., oxygen and Fe(III)) for U(IV) are usually concurrently present, which may cause fast remobilization of U if oxidants re-enter bioreduction zones once electron-donor additions cease. However, natural reductants present, such as reduced minerals and biomass, may enhance the longevity of noncrystalline U(IV) against oxidation by scavenging oxidants. It is therefore critical to understand the reactivity of noncrystalline U(IV) and its potential mobilization pathways during redox transitions under environmentally relevant conditions.

During reductive bioremediation, iron sulfide minerals (e.g., mackinawite; hereafter referred to as FeS) are commonly reported

Received: September 3, 2015
Revised: November 24, 2015
Accepted: December 22, 2015
Published: December 22, 2015

DOI: 10.1021/acs.est.5b04281
Environ. Sci. Technol. 2016, 50, 1403−1411

by-products along with U(IV) precipitates.[11,18,19] Previous studies have conclusively demonstrated that FeS is capable of both reducing uranyl ion[20,21] and inhibiting UO_2 oxidative dissolution by scavenging DO.[22,23] Field studies attributed the retardation of U mobilization to sulfide minerals formed in the subsurface environment.[18,24] Because FeS was also found in close association with noncrystalline U(IV) in biostimulated aquifers,[11] the protection of the U(IV) species against oxidation was expected. However, given the lability of noncrystalline U(IV),[16,17] it is unclear whether oxygen will preferentially react with FeS to limit the oxidative mobilization of this U(IV) species. In addition, because FeS oxidation by oxygen generates a number of Fe(III) products, the newly formed Fe(III) species may act as additional oxidants to cause U(IV) oxidation and mobilization. Although Fe(III) products were not observed to oxidize UO_2 during FeS oxidation,[25] the thermodynamic favorability may be shifted toward the oxidation of noncrystalline U(IV).[26,27] The role of FeS in influencing the stability of noncrystalline U(IV) can therefore be different from that of UO_2.

The objective of this study was to determine the effect of FeS on the oxidative mobilization of noncrystalline U(IV) under relevant oxic groundwater conditions controlled by the introduction of DO. Biomass-associated noncrystalline U(IV) suspensions were prepared in a medium that suppressed UO_2 formation. Laboratory flow-through experiments were conducted to investigate the change of U and Fe speciation as a function of carbonate concentration and solution pH. Surface-sensitive X-ray photoelectron spectroscopy (XPS) was employed to characterize intermediate U and Fe oxidation products. The amount of U release versus time was also determined to obtain U oxidation rate, which was compared with that of UO_2 under similar experimental conditions. The results obtained from this study contribute to a fundamental understanding of the reactivity of noncrystalline U(IV) species and their resistance to reoxidation in natural and bioremediated sediments.

MATERIALS AND METHODS

Synthesis of Mackinawite and Noncrystalline U(IV). Mackinawite was synthesized by mixing 1.1 M Na_2S solution with 0.57 M $FeCl_2$ solution (S:Fe ≈ 1.93) inside an anaerobic chamber with a gas composition of ∼5% H_2 in N_2.[22] The precipitate was allowed to age for 3 days under constant stirring before being rinsed with deoxygenated DI water. The final product was freeze-dried under a vacuum and stored in capped glass vials inside the anaerobic chamber until use. The resulting mackinawite was characterized as nanocrystalline particles with mineralogical description as detailed in Jeong et al.[28]

Biomass-associated noncrystalline U(IV) was produced as previously described in Bernier-Latmani et al.[7] Briefly, *Shewanella oneidensis* MR-1 cultures were grown anaerobically in sterile Luria−Bertani (LB) medium and harvested when they reached mid-exponential phase. Cells were harvested by centrifugation at 8000 *g* for 10 min and washed in simple BP medium, composed of 30 mM $NaHCO_3$ and 20 mM 1,4-piperazinediethanesulfonic acid (PIPES buffer) adjusted to pH 6.8. The reduction assay was initiated inside an anaerobic chamber by resuspending the washed cells in Widdel low phosphate (WLP) basal medium to an OD_{600} of 1 and amending it with 20 mM lactic acid and 1 mM uranyl acetate (Table S1). Subsamples of the suspension were collected and filtered, and the filtrate was analyzed by ICP-MS to confirm the complete removal of U(VI) in the aqueous phase. The cell suspensions were then collected by centrifugation, resuspended in a small volume of anoxic water, placed in serum bottles with a N_2 headspace, sealed within Mylar bags purged with N_2, and shipped from École Polytechnique Fédérale de Lausanne to the University of Michigan using an overnight delivery service. Characterization of this material by TEM and XAS confirmed that the reduced U(IV) was primarily in a form of noncrystalline U(IV) (Figure S1).

Oxidation of Noncrystalline U(IV) in Flow-Through Systems. The oxic flow-through experiments were conducted with 50 mL continuously stirred tank reactors (CSTRs) (Figure S2) using an initial ∼0.46 mM noncrystalline U(IV). At the beginning of an experiment, 4.8 mM FeS (0.43 g/L) was added to the CSTR reactor in an anaerobic chamber to provide a FeS:U(IV) molar ratio of ∼10, representing a lower-end ratio in the field.[11] An influent solution containing varing concentrations of $NaHCO_3$, KCl, and $CaCl_2$ was prepared and constantly purged with an $O_2/CO_2/N_2$ gas mixture to obtain the desired pH, dissolved oxygen (DO), and total inorganic carbonate (DIC) concentrations (Table S2). To study the impact of carbonate on noncrystalline U(IV) oxidation, we varied both $NaHCO_3$ concentration and P_{CO_2} in the gas mixture while keeping the solution pH constant at 7.0 ± 0.1. For the experiments without carbonate, 10 mM 3-(*N*-morpholino) propanesulfonic acid (MOPS, pK_a = 7.2) was used to buffer pH at 7.0. The resulting influent DIC concentration ranged from 0 to 10.8 mM. The oxic influent (∼1.8 mg·L^{-1} DO) was delivered to the reactors by a peristaltic pump at a rate of 1.8−2.0 mL·min^{-1} until complete FeS oxidation had occurred. Effluent DO, pH, and Eh were constantly monitored to track the process of FeS oxidation. All oxic flow-through experiments were operated outside the anaerobic chamber at room temperature (23 ± 1 °C) and covered by aluminum foil to avoid light exposure. Control experiments of noncrystalline U(IV) oxidation in the absence of FeS were conducted under otherwise identical experimental conditions. To determine the oxidation rate of noncrystalline U(IV) under anoxic conditions, we operated the entire flow-through system in an anaerobic chamber in the presence and absence of FeS. The influent solution was prepared with deoxygenated DI water and purged with oxygen-free gas to ensure consistently anoxic conditions (<0.1 mg·L^{-1} DO).

To test the role of FeS oxidation products on noncrystalline U(IV) mobilization, we conducted flow-through experiments at both acidic (5.4) and basic (9.0) pH values. Previous studies demonstrated that FeS oxidized through pH-dependent reaction pathways: proton-promoted solution-phase oxidation at acidic pH and surface-mediated oxidation at basic pH.[23,29] Distinct intermediate Fe(III) products may be generated at different pH values,[29] affecting the stability of noncrystalline U(IV) through redox reactions. Influent chemical compositions were modified for basic pH experiments (Table S2) to maintain DIC concentrations at ∼1 mM and prevent calcite precipitation.

To test the effect of aging of FeS oxidation products, we used two types of model compounds for the flow-through experiments. We synthesized two-line ferrihydrite (5.1 mM total Fe) according to Schwertmann and Cornell[30] to represent an early-stage FeS oxidation model product that could potentially oxidize noncrystalline U(IV). A Fe(III) solid mix was also prepared by oxidizing FeS in a batch reactor with

DOI: 10.1021/acs.est.5b04281
Environ. Sci. Technol. 2016, 50, 1403−1411

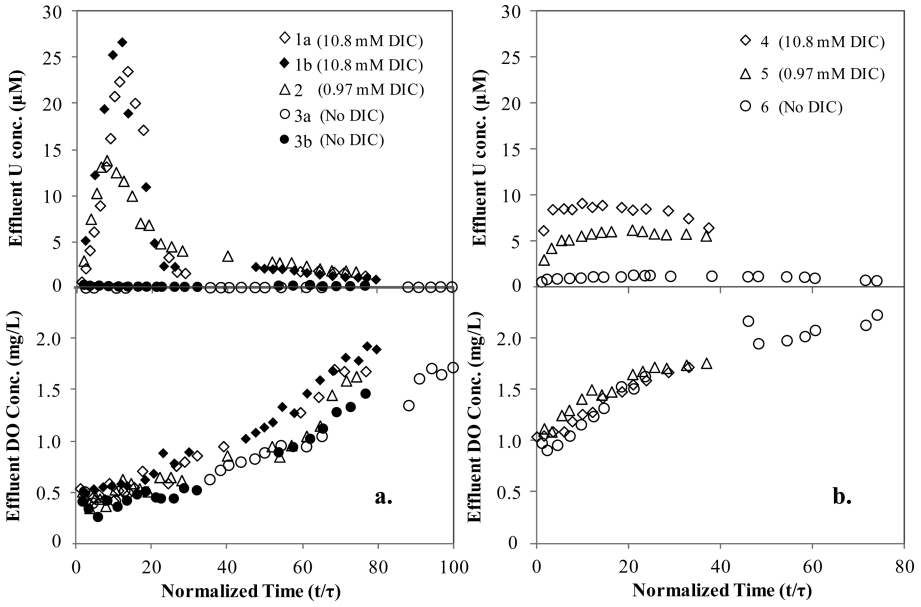

Figure 1. Total dissolved U and dissolved oxygen (DO) concentration profiles as a function of time during the oxidative mobilization of ~0.47 mM noncrystalline U(IV) in the presence (a) and absence (b) of 4.8 mM FeS. Replicates are represented by the filled vs open symbols. Influent solution condition: 0.4 mM KCl, and 2.0 mM $CaCl_2$, 1.8 mg·L^{-1} influent DO, and pH 7.0.

oxygen to represent the aged Fe(III) products. The matrix (4.4 mM total Fe) was previously characterized to consist of goethite, lepidocrocite, and elemental sulfur.[22]

Analyses. Total dissolved Fe and U were determined in effluent samples by ICP-MS (Agilent 7900). The detection limits for U and Fe were 0.01 and 0.1 $\mu g \cdot L^{-1}$, respectively. Dissolved Fe(II) was determined photometrically by the ferrozine method at 562 nm using a UV/vis spectrophotometer (Varian Cary 3E). The dissolved Fe(II) equaled total dissolved Fe measured by ICP-MS within 5% error. Because aqueous sulfide, thiosulfate, and sulfate were previously determined to be negligible during the abiotic oxidation reaction,[22,23] these sulfur species were not measured in the present study.

In selected flow-through experiments, solid suspensions were collected at various time points for analyzing the change of oxidation state and stoichiometry of U. The CSTR reactor was quickly transferred to the anaerobic chamber, where a 1−2 mL suspension sample was taken. The flow was briefly interrupted for less than 5 min before the oxidation reaction was resumed. The solid samples were then characterized by XPS at the University of Michigan Electron Microbeam Analysis Laboratory (EMAL). Briefly, wet pastes obtained after filtering through a 0.1 μm nylon membrane were dried in the anaerobic chamber and mounted on double-sided Cu tape. The samples, kept inside airtight containers, were transferred to the XPS chamber. XPS spectra were collected on a Kratos Axis Ultra XPS using a monochromated Al−K_α X-ray source (1486 eV). Region scans were obtained for U 4*f* peaks, Fe $2p_{3/2}$, and S 2*p*, with the energy calibrated to adventitious C 1s at a binding energy of 284.5 eV. Spectra were best fit by nonlinear least-squares with a Gaussian−Lorentzian peak using the CasaXPS curve resolution software. Mass balance of U was checked at the end of the experimental run for selected samples. To do this, when the experiment was completed, we digested solid samples in CSTR in concentrated nitric acid to determine solid-bound U concentration and added to the total amount that had exited the reactor.

Oxidation Rate Calculations. When noncrystalline U(IV) was rapidly oxidized by DO, effluent U concentration versus time profiles displayed a sharp U peak without reaching steady state. The oxidation rate was estimated by the amount of total U released into the effluent within a given time. The cumulative total U release was based on measured U concentration and flow rate and was plotted against reaction time (Figure S3). The oxidation rates R_n (mol·mol U(IV)$^{-1}$·s^{-1}) for noncrystalline U(IV) were obtained by subjecting the initial linear portion of the plots to regression analysis, followed by a normalization with respect to the total mole of noncrystalline U(IV). Because the noncrystalline U(IV) had an unclear chemical composition and structure, molar concentration was used for rate calculation instead of mass concentration. For the rate analysis, typically more than seven points were utilized, resulting in R^2 values greater than 0.98 for all least-squares fits. Because noncrystalline U(IV) may contain up to 10% U(VI) as estimated by XPS, the potential contribution of U(VI) to the overall U release was subtracted from initial rates described above. The influence of U(VI) component on the oxidation rates was reflected in the error bar: the upper limit showed the oxidation rate of noncrystalline U(IV) without any U(VI) impurity, while the lower limit showed the rate with 10% U(VI) impurity.

In cases in which a steady-state effluent U concentration was established relatively quickly after an initial reactor start-up, the oxidation rate of noncrystalline U(IV) (R_n) was calculated using the following eq (eq 1):

$$R_n = \frac{[U]_{ss} \times Q}{V \times [U(IV)_{noncrystalline}]} \quad (1)$$

where R_n (mol·mol U(IV)$^{-1}$·s^{-1}) is mass-normalized oxidation rate of noncrystalline U(IV), Q (L·s^{-1}) the flow rate, V (L) the reactor volume, $[U]_{ss}$ (mol·L^{-1}) the steady-state concentration of total dissolved U, and $[U(IV)_{noncrystalline}]$ (mol U(IV)·L^{-1}) the molar concentration of noncrystalline U(IV) in the reactor. The $[U]_{ss}$ was typically the average of the values from periods of 10 or more residence times, over which the effluent U

DOI: 10.1021/acs.est.5b04281
Environ. Sci. Technol. 2016, 50, 1403−1411

Table 1. Experimental Mole-Normalized Oxidation Rates (R_n) of Noncrystalline U(IV) Obtained under Various Combinations of Oxidizing Conditions and Water Compositions

experimental ID	[noncrystalline U(IV)] (mM)	[FeS] (mM)	pH	DO ($mg \cdot L^{-1}$)	DIC[a] (mM)	flow rate ($mL \cdot min^{-1}$)	$[U]_{ss}$[b] (μM)	$R_n \times 10^{-6}$ (mol U·mol $U(IV)^{-1} \cdot s^{-1}$)
variation of carbonate								
1a	0.46	4.8	7.0	1.8	10.8	1.89	\	25.5 ± 4.14
1b	0.47	4.8	7.0	1.8	10.8	1.83	\	23.8 ± 3.86
2	0.47	4.8	7.0	1.8	0.97	1.86	\	13.7 ± 1.84
3a	0.47	4.8	7.0	1.8	0	1.88	0.12	0.16 ± 0.01
3b	0.47	4.8	7.0	1.8	0	1.81	0.10	0.13 ± 0.01
4	0.46	\	7.0	1.8	10.8	1.84	8.63	11.5 ± 0.23
5	0.47	\	7.0	1.8	0.97	1.81	5.93	7.61 ± 0.17
6	0.47	\	7.0	1.8	0	1.81	1.25	1.66 ± 0.06
variation of DO								
7	0.48	4.8	7.0	<0.1	10.8	1.83	0.076	0.099 ± 0.004
8	0.46	\	7.0	<0.1	10.8	1.91	1.42	1.96 ± 0.05
variation of pH								
9	0.47	4.8	5.4	1.8	1.8	1.90	\	2.30 ± 0.21
10	0.47	4.8	9.0	1.8	1.0	1.88	\	22.1 ± 3.31
11	0.47	\	5.4	1.8	1.8	1.91	6.41	8.88 ± 0.42
variation of Fe(III) oxides								
12	0.45	Goe.	7.0	1.8	10.8	1.96	9.06	12.3 ± 0.32
13	0.51	Ferri.	7.0	1.8	10.8	1.84	11.4	14.7 ± 0.65

[a]Dissolved inorganic carbon (DIC) calculated from Visual MINTEQ at equilibrium with CO_2 gas mix used (Table S2). [b]When steady-state oxidation of noncrystalline U(IV) was observed, eq 1 was used to calculate the corresponding oxidation rate.

concentration varied by less than 10%. Over 40 residence times (equivalent to ~18 h) in such a flow-through experiment, usually less than 40% of total noncrystalline U(IV) was oxidized and dissolved. The mass concentration of noncrystalline U(IV) at steady-state oxidation was then adjusted for the loss of U from the reactor in rate calculations.

RESULTS AND DISCUSSION

FeS Failure to Inhibit the Rapid Oxidation of Noncrystalline U(IV) in the Presence of Carbonate. The oxidation of noncrystalline U(IV) was examined in the presence of 4.8 mM FeS under varied total carbonate concentration ranging from 0 to 10.8 mM. Contrary to the expectation that FeS would effectively consume oxygen and inhibit noncrystalline U(IV) oxidation, dissolved U rapidly increased upon the introduction of an oxic solution to the CSTR (Figure 1a). The oxidation of noncrystalline U(IV) showed a clear dependence on total dissolved carbonate (DIC) concentration of the influent. With 10.8 mM DIC, total dissolved U concentration peaked at ~25 μM within 13 residence times (τ) (equivalent to ~5 h). A lower peak value of ~14 μM occurred at a DIC concentration of 0.97 mM. In the absence of carbonate, a much slower oxidation of noncrystalline U(IV) was observed throughout the course of the experiment, where the dissolved U concentration remained less than 0.3 μM. The calculated oxidation rate of noncrystalline U(IV) dropped considerably from 25×10^{-6} to $\sim 0.15 \times 10^{-6}$ (mol·mol $U(IV)^{-1} \cdot s^{-1}$) as DIC concentration decreased from 10.8 mM to 0 mM (Table 1). In contrast, DO concentration profiles followed a similar trend at different DIC concentrations despite the discrepancy in the oxidation of biomass-associated noncrystalline U(IV). The effluent DO concentrations steadily increased after 20 τ in all experiments until the influent level (~1.8 $mg \cdot L^{-1}$) was reached after a brief stagnancy at ~0.5 $mg \cdot L^{-1}$. Evidently, although FeS was able to remove DO in the suspension, the mobilization of U was not inhibited by its presence. The fast release of U was not captured by effluent Eh, which resembled the trend of DO (data not shown).

The lack of inhibition on U mobilization by FeS (Figure 1a) suggested that noncrystalline U(IV) can be easily oxidized by DO at low concentrations. The subsequent mobilization of oxidized U(VI) depended on carbonate concentration in the oxic solution. To examine the influence of oxygen and carbonate levels on the oxidation of noncrystalline U(IV), we conducted control experiments without FeS using influent solutions containing the same DO (1.8 $mg \cdot L^{-1}$) and a range of carbonate concentration (0–10.8 mM). Figure 1b shows that a higher DIC concentration resulted in a greater release of dissolved U to the effluent. However, the dramatic rise in U concentration (Figure 1a) was not observed in any control experiment, even though the DO levels were higher than those in the presence of FeS. Steady-state oxidation of noncrystalline U(IV) was quickly established at relatively low U concentrations. The steady-state U concentrations were then used to calculate the oxidation rates of noncrystalline U(IV), which increased from 1.66 to 11.5×10^{-6} (mol·mol $U(IV)^{-1} \cdot s^{-1}$) as DIC concentration rose. Compared with the rates in the presence of FeS, noncrystalline U(IV) dissolved approximately 50% more slowly at high DIC concentrations (>0.1 mM). At 0 mM DIC, however, the oxidation rate in the absence of FeS was ~10 times greater than that in the presence of FeS.

Although both DO and carbonate promoted the oxidation of noncrystalline U(IV), the U peak exhibited in Figure 1a cannot be explained solely by these two factors. FeS seems to play a critical but unexpected role in influencing U mobilization upon oxygen intrusion. The results are noticeably different from the inhibited oxidative dissolution of UO_2 by FeS as discussed in previous studies.[22,23] The dissolution rate of synthetic UO_2 is approximately an order of magnitude lower in the presence of FeS under similar conditions due to effective removal of oxygen (Figure 2). Extensive dissolution of UO_2 occurred only when FeS was depleted and DO levels started to increase.[25] FeS was

DOI: 10.1021/acs.est.5b04281
Environ. Sci. Technol. 2016, 50, 1403–1411

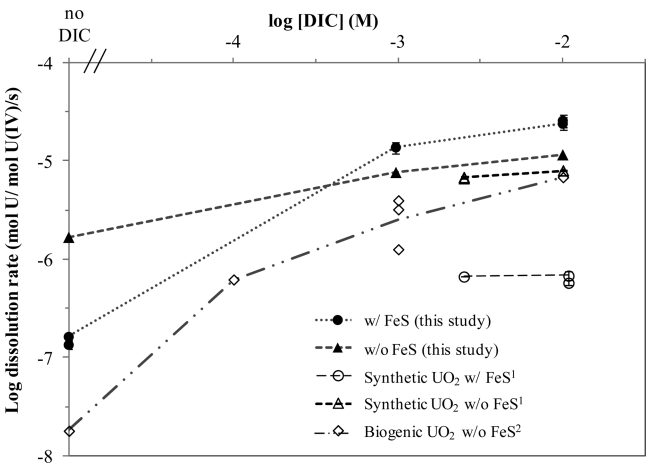

Figure 2. Log-mole-normalized oxidation rates (mol·mol U(IV)$^{-1}$·s^{-1}) of noncrystalline U(IV) determined under moderately oxidizing conditions (1.8 mg·L^{-1} DO) as a function of total DIC concentration in the presence and absence of FeS at pH 7.0. The rates are compared with previously reported values obtained from chemogenic[23] and biogenic[43] UO_2 particles under similar experimental conditions.

identified as an effective oxygen scavenger without the ability to enhance U mobilization. The more rapid oxidation of noncrystalline U(IV) in the presence of FeS may be due to the catalytic role of oxidized FeS in facilitating electron transfer, as discussed in the sections below.

Figure 2 also demonstrates that the dissolution rate of UO_2 is slower than that of noncrystalline U(IV) regardless of carbonate concentration under oxic conditions, which agrees with a previous batch study using an air-saturated solution.[17] The difference in mobilization between the two reduced U(IV) species points to the inherent difference in reactivity between the species. Because of the absence of a crystalline structure, noncrystalline U(IV) seems susceptible to oxidation even at relatively low DO levels (<0.5 mg·L^{-1}). Importantly, dissolved carbonate promotes the oxidative mobilization of both reduced U(IV) species,[25,31] suggesting that carbonate facilitates the release of U(VI) products to the bulk solution in similar manners.

Oxidation of Noncrystalline U(IV) by Oxidized FeS. In previous studies, FeS was identified as an oxygen scavenger and reductant for U(VI) to inhibit the dissolution of crystalline UO_2 in oxic groundwater.[21,23] The fast oxidation of noncrystalline U(IV) in the current study (Figure 1a), however, suggests a complex role of FeS in influencing U mobilization. To further elucidate its role, we conducted experiments under anoxic conditions in the presence and absence of FeS. The results (Figure S4) show that dissolved U concentrations were significantly lower (<0.1 μM) with 4.8 mM FeS than the control (~1.3 μM) without FeS at steady state. Concomitantly, the oxidation rate of noncrystalline U(IV) decreased from 1.96 × 10^{-6} (without FeS) to 0.099 × 10^{-6} (mol·mol U(IV)$^{-1}$·s^{-1}) (with FeS), excluding the possibility that FeS intrinsically promoted U mobilization (Table 1). The inhibitory effect of FeS under anoxic conditions may be attributed to the adsorption of dissolved U(IV) species to FeS particles, given the large surface areas provided by the disordered FeS.[28,32] However, the inhibited mobilization of noncrystalline U(IV) cannot be sustained once FeS is oxidized by oxygen, particularly when the carbonate level is relatively high. Therefore, it is plausible that the oxidation products of FeS catalyzed the oxidative mobilization of noncrystalline U(IV), given FeS can transform to a range of redox reactive Fe(III) species after oxidation.[22,29]

To examine the potential of Fe(III) species for oxidizing noncrystalline U(IV), we determined effluent Fe(II) concentrations from flow-through experiments in the presence of FeS. As shown in previous studies, FeS dissolved under oxic conditions as a result of oxidative dissolution and preferential release of ferrous iron.[33,34] Depending on the solution pH, FeS oxidation also led to the formation of various Fe(III) (hydr)oxides, including ferrihydrite, goethite, lepidocrocite, and green rust.[22,29] If the Fe(III) species can react with noncrystalline U(IV), higher concentrations of dissolved Fe(II) would be generated relative to background Fe(II). With only FeS (Figure 3), a peak concentration for dissolved Fe(II) of

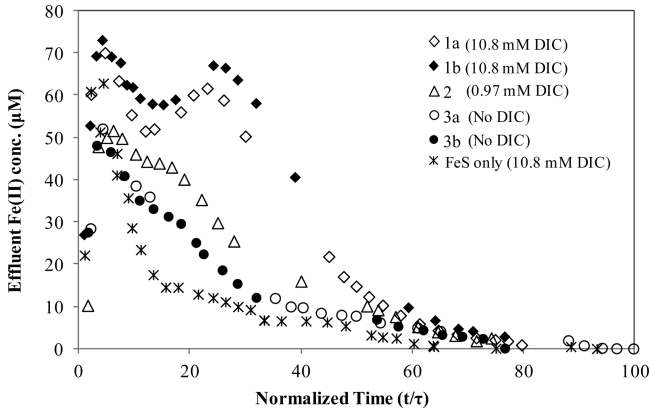

Figure 3. Release profiles of dissolved Fe(II) from FeS as a function of time at different influent carbonate concentrations in the presence and absence of noncrystalline U(IV). The experimental ID and corresponding carbonate concentrations are labeled. All influent solutions had a DO concentration of 1.8 mg·L^{-1} and a pH of 7.0. Replicates are represented by the filled vs open symbols.

~60 μM was rapidly established after ~5 τ, which then continuously decreased until complete FeS oxidation. This background Fe(II) profile agreed with previous studies at pH 7,[23] showing a loss of ~18% of total Fe(II) to the effluent. In the presence of noncrystalline U(IV), however, dissolved Fe(II) remained at a high concentration (~60 μM) for an additional ~30 τ after the peak at ~6 τ in 10.8 mM DIC solution. By integrating the area below the Fe(II) profile, we estimated the total released Fe(II) during the course of oxidation to be ~56% of total Fe(II) in FeS. With a decreasing carbonate concentration, the amount decreased to 33% and 26% in 0.97 mM and 0 mM DIC solutions, respectively. Clearly, more dissolved Fe(II) coincided with the greater oxidation rate of noncrystalline U(IV). The greater production of dissolved Fe(II) likely resulted from the reduction of Fe(III) by noncrystalline U(IV), although the specific Fe(III) phases remained to be characterized. This result points to the possibility of Fe(II) redox cycling during the oxidative mobilization of U(IV). Consistent with this notion, the redox couples of U(IV)/U(VI) and Fe(II)/Fe(III) (hydr)oxide have similar electrode potentials under common groundwater conditions.[26,35] Although the geochemical conditions did not favor UO_2 oxidation in a previous study,[25] biomass-associated noncrystalline U(IV) in molecular forms may be susceptible to oxidation by Fe(III) species. Given these results, this study provides compelling causative evidence that Fe(III) products

DOI: 10.1021/acs.est.5b04281
Environ. Sci. Technol. 2016, 50, 1403−1411

from FeS oxidation can play a significant role in oxidizing and mobilizing the bioreduced form of U during redox transitions.

Under acidic pH, FeS was substantially dissolved to generate more dissolved Fe(II) in effluent. The proton-promoted solution-phase oxidation of FeS at pH 5.4 resulted in a release of over 85% of total Fe and minor Fe(III) formation in the CSTR (Figure S5). This different FeS oxidation pathway also affected the oxidation of noncrystalline U(IV). Without exhibiting a high peak concentration, dissolved U(VI) remained relatively low (~1.6 μM) for 30 τ (Figure S6). Even after oxygen breakthrough at ~60 τ, the U concentration never exceeded 5 μM. In contrast, the experiment conducted at pH 9 showed a similar trend of U mobilization as in Figure 1, where significant release of U occurred immediately after oxygen introduction. The results suggest that oxidative mobilization of noncrystalline U(IV) may strongly depend on Fe solid-phase species produced from FeS oxidation. Only solid-associated Fe(III) species (i.e., bulk or surface-adsorbed Fe(III)) may act as effective oxidants for noncrystalline U(IV). However, it should be noted that neither aged Fe(III) products nor synthetic 2-line ferrihydrite solids has a comparable reactivity as freshly oxidized FeS for mobilizing noncrystalline U(IV) under the same flow-through experimental conditions (Figure S7). In both experiments, U mobilization exhibited a steady-state profile, similar to the control experiment in the absence of Fe solids. Therefore, the reactive Fe(III) species capable of oxidizing noncrystalline U(IV) was probably an intermediate Fe(III) produced at the early stage of FeS oxidation.

Characterization of U and Fe Species during Oxidation. To elucidate the mechanism for the promoted oxidative mobilization of noncrystalline U(IV) by FeS, we conducted XPS analyses on solid samples collected within the initial 15 τ of flow-through experiments at pH 7 (Table 2).

Table 2. U 4f XPS Fitting Parameters and Relative Concentrations of U(IV), U(V), and U(VI) Components Determined by XPS on Selected Flow-through Experimental Samples Containing Biomass-Associated Noncrystalline U(IV)

reaction time (t/τ)	peak U(IV) $4f_{7/2}$ (eV)	fwhm[a]	U(IV) (%)	U(V) (%)	U(VI) (%)
experiment no. 1 with 10.8 mM DIC and 4.8 mM FeS					
0	379.8	1.67	88	2	10
5	379.6	1.98	17	9	74
13	379.9	1.89	68	7	25
experiment no. 3 with 0 mM DIC and 4.8 mM FeS					
5	379.8	2.25	26	0	74
15	379.9	2.42	67	9	24
experiment no. 4 with 10.8 mM DIC, no FeS					
6	379.8	1.69	89	2	9

[a]Full width at half-maximum of fitted U components on U 4f XPS spectra. All three U components are constrained to have the same fwhm in a spectrum.

Detailed characterization with XPS provided a direct investigation on the oxidation states of Fe and U at or near surface of solid mixtures. Because noncrystalline U(IV) is essentially biomass-associated U(IV) without crystal structure, the U components determined by XPS indicate the overall U speciation. Before oxidation was initiated, the noncrystalline U(IV) consisted of a small but measurable U(VI) component (~10%) (Figure 4a), partly due to inadvertent exposure to oxygen during sample handling and analysis. Shortly after oxidation began (~5 τ), the U(VI) component dramatically increased in relative concentration in the presence of FeS, accounting for ~74% of total U. The binding energy (BE) of the U(VI) $4f_{7/2}$ peak shifted from 381.6 eV to a higher value of 382.7 eV, greater than previously reported values for U(VI) solids.[36] The U(VI) species produced by noncrystalline U(IV) oxidation may not represent the known crystalline U(VI) phases but rather labile U(VI)-carbonate complexes, which would explain the fast release of soluble U in the presence of 10.8 mM DIC. Surprisingly, the U(VI) species quickly diminished, dropping to merely ~24% by 13 τ when the dissolved U concentration reached its peak value (Figure 1a). The U species appeared to be restored to a reduced form by releasing oxidized U(VI) to the effluent. After this time point, dissolved U(VI) continued to decrease until noncrystalline U(IV) was depleted from the CSTR. In all U 4f XPS spectra, a peak featuring N 1s remained, suggesting a close association of noncrystalline U(IV) with biomass-related N compounds.

Corresponding to the U(VI) dominance at ~5 τ, the FeS surface was significantly oxidized for a brief period. The characteristic Fe(II)-S component at 206.9 eV on Fe $2p_{3/2}$ XPS[37] diminished from 34% to 13% of the initial FeS (Figure 4d,e). In contrast, the multiplets of Fe(III)-S components between 709 to 712 eV increased drastically from 42% to 70% of total surface Fe components (Table S3). The full width at half-maximum (fwhm) for all Fe components in the oxidized sample also grew relative to those of the initial FeS, likely due to the more abundant high-spin surface Fe^{3+} species.[38] This change in surface Fe species during the initial oxidation suggested either a rapid transformation of surface Fe(II) to Fe(III) species or a preferential loss of structural Fe(II) due to dissolution. Given that the dissolved Fe(II) concentration also peaked within 5 τ (Figure 3), the preferential release of dissolved Fe(II) likely contributed to a Fe(III)-rich surface. As oxidation proceeded to 13 τ, the Fe(III)-S components decreased in relative concentrations, along with growing Fe(II)-S and Fe(II)-O components. Therefore, surface characterization of both U 4f and Fe $2p_{3/2}$ identified substantially oxidized surface species at an early stage of oxidation. The mobilization of noncrystalline U(IV) probably resulted from its oxidation by the transient surface Fe(III) species that were in close contact with U(IV) in the completely mixed reactor. Without FeS and its oxidation products, U components fit by XPS (Figure S8a) remained identical to the initial material at 6 τ in the control experiment. The U(IV)-dominated species suggests an effective removal of U(VI) to bulk solution facilitated by carbonate during oxidation by oxygen in the absence of FeS. Compared with DO, the surface Fe(III) species are perhaps better catalyst to facilitate electron transfer, causing rapid U(VI) accumulation before newly formed U(VI)-carbonate complexes can be removed from the biomass.

In the absence of carbonate, the oxidation of noncrystalline U(IV) appeared to be inhibited by FeS, implying a lack of U oxidation (Figure 1). However, the U 4f XPS spectra (Figure S8b) indicated a U(VI) dominance at ~5 τ, similar to the result in the presence of 10.8 mM DIC. The U(VI) proportion then decreased to 24% by 15 τ, although only <1% of total U had been released into effluent. The characterization of surface Fe by XPS (not shown) agreed with those observed in Figure 4, suggesting that the formation of Fe(III)-rich surface was independent of carbonate concentration in solution. Therefore,

DOI: 10.1021/acs.est.5b04281
Environ. Sci. Technol. 2016, 50, 1403−1411

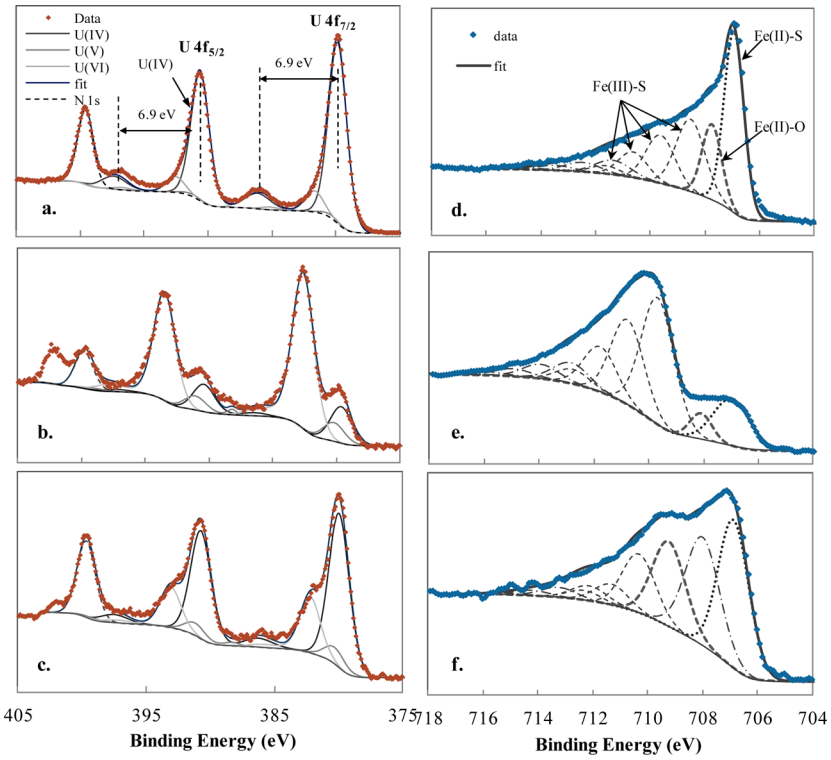

Figure 4. Narrow scans of U 4f (a,b,c) and Fe $2p_{3/2}$ (d,e,f) XPS spectra of solid samples collected as a function of time from flow-through experiment using 0.47 mM noncrystalline U(IV) and 4.8 mM FeS. (a) and (d): Initial materials before the start of oxidation; (b) and (e): 5 τ in experiment 1a; (c) and (f): 13 τ. All experiments were carried out under influent DO of 1.8 mg·L^{-1} and 10.8 mM DIC artificial groundwater conditions. The dots and colored solid lines are the experimental data and the corresponding fits, respectively.

noncrystalline U(IV) can be quickly oxidized by an intermediate Fe(III) species regardless of influent carbonate. The high concentration of effluent dissolved U, however, was accomplished only when a rapid release of U(VI) carbonate species occurred following the oxidation.

Complexity of Fe(III) Catalyzed Mobilization of Noncrystalline U(IV). The fast mobilization of noncrystalline U(IV) in this study identifies a transient Fe(III) species as a prominent oxidant for biomass-associated U(IV). The ferric iron is shown to be more effective than DO in extracting electrons from U(IV) and causing U(VI) accumulation over a short period of time. Stumm and co-workers have shown that electron-transfer reactions involving Fe(II) and Fe(III) are often accelerated as a results of specific adsorption of the metal cations to mineral surfaces.[39] Although the nature of the Fe(III) species remains unclear, XPS and flow-through results suggest that Fe(III) is likely bound to structural S(−II) on the FeS surface. After reacting with noncrystalline U(IV), the >Fe(III)-S species is reduced and released to the effluent as soluble Fe(II) (Figure 3). The fact that this Fe(III) species is short-lived and unsustainable over the oxidation of FeS possibly results from (1) the precipitation of less reactive Fe(III) (hydr)oxides solids, and (2) the formation of polysulfide and elemental sulfur.[40] Under acidic pH conditions, the slow oxidation of noncrystalline U(IV) (Figure S5) further implies the complexity of geochemical conditions affecting Fe(III) speciation. One possible explanation is the lack of Fe(III) surface species at a pH of ∼5 owing to the slow oxidation kinetics of dissolved Fe(II).[41] The oxidation rate of noncrystalline U(IV) is limited relative to the control experiment in the absence of FeS (Table 1), likely because surface Fe(III) is absent or negligible, and DO levels are lowered by FeS consumption. Therefore, the pH-dependent oxidation pathway of FeS has potentially an important impact on noncrystalline U(IV) oxidation. From neutral to basic pH values, the surface-mediated oxidation pathway becomes increasingly dominant,[29] where structural Fe(II) in FeS is oxidized on solid surface without dissolving into the bulk solution. Although transitory, the reactive surface Fe(III) species may be more abundant at higher pH, contributing to the faster release of U at a given carbonate concentration.

During the rapid oxidative mobilization of noncrystalline U(IV), soluble carbonate plays an critical role by forming stable complexes with U(VI) and facilitating the release of U(VI) from a biomass matrix, which includes cell membranes, lysed cellular material, and exopolymeric substances. Thus, the limited oxidation of noncrystalline U(IV) (Figure 1a) appears plausible once DIC is removed from the influent. In the absence of carbonate, oxidized U cannot form highly soluble complexes, and it may be effectively adsorbed by FeS or remain bound to the biomass via chemical bonds with organic ligands. Intriguingly, oxidized U(VI) may even become reduced again by FeS after 5 τ as suggested by the XPS result (Figure S8c). Given that more than 99% of U remains solid-bound at 0 mM DIC, the recovery of U(IV) implies that FeS acts as an effective reductant for surface-adsorbed and biomass-associated U(VI) upon slight oxidation. These results are also supported by previous reports showing that FeS reduced U(VI) to U(IV) species in the absence of carbonate.[21,42] Until FeS depletion and oxygen breakthrough, the dissolved U concentration is kept relatively low (Figure 1a), possibly due to readsorption of soluble U(VI) to Fe(III) (hydr)oxides generated from FeS oxidation. Overall, noncrystalline U(IV) has demonstrated a high susceptibility to oxidation in a FeS-containing system

DOI: 10.1021/acs.est.5b04281
Environ. Sci. Technol. 2016, 50, 1403−1411

upon oxygen invasion, likely inherent to its molecular form and relatively weak association with biomass ligands. The eventual mobilization of U(VI), however, is caused by a combination of complexation, adsorption, and redox reactions, which are strongly influenced by the geochemical conditions (i.e., pH, DIC, DO, etc.).

Environmental Implications. The long-term success of in situ biostimulated U(VI) immobilization relies on the stability of reduced U(IV) (i.e., noncrystalline U(IV) and uraninite) under redox fluctuating conditions, such as when oxygen reenters the active treatment zone. This study demonstrates that biomass-associated noncrystalline U(IV) is more readily oxidized than UO_2 following oxygen intrusion under simulated groundwater conditions. While effectively consuming oxygen, FeS may indirectly accelerate U mobilization through the formation of reactive intermediate Fe(III) surface species that promote electron transfer and oxidation of U(IV). The resulting U mobilization is further promoted by the presence of carbonate, which forms stable complexes with U(VI) and facilitates the detachment from biomass. Because both iron sulfides and carbonate are commonly encountered in a groundwater system, the oxidative mobilization of bioreduced U(IV) species may occur at a faster rate than predicted on the basis of current oxidative dissolution studies and associated geochemical models assuming the sole existence of crystalline UO_2. This vulnerability may also in part explain the "unexpectedly" fast remobilization of bioreduced U(IV) in sediment columns once electron donor additions are halted.[12] Given the sparsity of thermodynamic and kinetic data on redox reactions of noncrystalline U(IV), more work is needed to evaluate the scale of its abundance and capture its lability in geochemical models. Whereas most recent studies focus on resolving U(IV) speciation, even less is known about the potential transformation of noncrystalline U(IV) species to more crystalline UO_2. Conditions that favor the preferential formation of UO_2 over noncrystalline U(IV) would allow a more effective inhibition of U(IV) oxidation by iron sulfides and prolonged U immobilization in the event of occasional oxygen intrusion into reducing zones. Future research should examine the mechanisms of U retention and rates of oxidative remobilization in natural sediments where FeS are produced with mixed U(IV) species.

■ ASSOCIATED CONTENT

Supporting Information

The Supporting Information is available free of charge on the ACS Publications website at DOI: 10.1021/acs.est.5b04281.

Tables showing the WLP media composition (Table S1), artificial groundwater compositions (Table S2), and Fe 2p3/2 XPS fitting results (Table S3). Figures showing noncrystalline U(IV) characterization (Figure S1), flow-through system schematic (Figure S2), cumulative U release for rate analysis (Figure S3), anoxic dissolution of noncrystalline U(IV) (Figure S4), final oxidation products (Figure S5), pH-dependent oxidation of noncrystalline U(IV) (Figure S6); effect of Fe(III) on U(IV) oxidation (Figure S7), and U 4f XPS spectra (Figure S8). (PDF)

■ AUTHOR INFORMATION

Corresponding Author

*Tel: (734) 764-8495; fax: (734) 763-2275; e-mail: ford@umich.edu.

Notes

The authors declare no competing financial interest.

■ ACKNOWLEDGMENTS

The authors would like to thank Tom Yavaraski for his technical assistance in ICP-MS sample analysis. We also thank Young-Soo Han at the Korea Institute of Geoscience and Mineral Resources for her help with the XPS analysis. This research was supported by Subsurface Biogeochemical Research Program in the Office of Science (BER), U.S. Department of Energy, grant no. DE-FG02-09ER64803. Part of this research was carried out at SSRL, a Directorate of SLAC National Accelerator Laboratory and an Office of Science User Facility operated for the U.S. DOE by Stanford University. Work at EPFL was funded by grant no. 200020-144335 from the Swiss National Science Foundation.

■ REFERENCES

(1) Wall, J. D.; Krumholz, L. R. Uranium Reduction. *Annu. Rev. Microbiol.* **2006**, *60* (1), 149−166.

(2) Lovley, D. R.; Phillips, E. J. P.; Gorby, Y. A.; Landa, E. R. Microbial reduction of uranium. *Nature* **1991**, *350* (6317), 413−416.

(3) Abdelouas, A.; Lutze, W.; Gong, W.; Nuttall, E. H.; Strietelmeier, B. A.; Travis, B. J. Biological reduction of uranium in groundwater and subsurface soil. *Sci. Total Environ.* **2000**, *250* (1−3), 21−35.

(4) Gu, B.; Wu, W.-M.; Ginder-Vogel, M. A.; Yan, H.; Fields, M. W.; Zhou, J.; Fendorf, S.; Criddle, C. S.; Jardine, P. M. Bioreduction of uranium in a contaminated soil column. *Environ. Sci. Technol.* **2005**, *39* (13), 4841−4847.

(5) Lovley, D. R.; Roden, E. E.; Phillips, E. J. P.; Woodward, J. C. Enzymatic iron and uranium reduction by sulfate-reducing bacteria. *Mar. Geol.* **1993**, *113* (1−2), 41−53.

(6) Bargar, J. R.; Bernier-Latmani, R.; Giammar, D. E.; Tebo, B. M. Biogenic uraninite nanoparticles and their importance for uranium remediation. *Elements* **2008**, *4* (6), 407−412.

(7) Bernier-Latmani, R.; Veeramani, H.; Vecchia, E. D.; Junier, P.; Lezama-Pacheco, J. S.; Suvorova, E. I.; Sharp, J. O.; Wigginton, N. S.; Bargar, J. R. Non-uraninite products of microbial U(VI) reduction. *Environ. Sci. Technol.* **2010**, *44* (24), 9456−9462.

(8) Veeramani, H.; Alessi, D. S.; Suvorova, E. I.; Lezama-Pacheco, J. S.; Stubbs, J. E.; Sharp, J. O.; Dippon, U.; Kappler, A.; Bargar, J. R.; Bernier-Latmani, R. Products of abiotic U(VI) reduction by biogenic magnetite and vivianite. *Geochim. Cosmochim. Acta* **2011**, *75* (9), 2512−2528.

(9) Fletcher, K. E.; Boyanov, M. I.; Thomas, S. H.; Wu, Q. Z.; Kemner, K. M.; Loffler, F. E. U(VI) reduction to mononuclear U(IV) by desulfitobacterium species. *Environ. Sci. Technol.* **2010**, *44* (12), 4705−4709.

(10) Boyanov, M. I.; Fletcher, K. E.; Kwon, M. J.; Rui, X.; O'Loughlin, E. J.; Löffler, F. E.; Kemner, K. M. Solution and microbial controls on the formation of reduced U(IV) species. *Environ. Sci. Technol.* **2011**, *45* (19), 8336−8344.

(11) Bargar, J. R.; Williams, K. H.; Campbell, K. M.; Long, P. E.; Stubbs, J. E.; Suvorova, E. I.; Lezama-Pacheco, J. S.; Alessi, D. S.; Stylo, M.; Webb, S. M.; Davis, J. A.; Giammar, D. E.; Blue, L. Y.; Bernier-Latmani, R. Uranium redox transition pathways in acetate-amended sediments. *Proc. Natl. Acad. Sci. U. S. A.* **2013**, *110* (12), 4506−4511.

(12) Sharp, J. O.; Lezama-Pacheco, J. S.; Schofield, E. J.; Junier, P.; Ulrich, K.-U.; Chinni, S.; Veeramani, H.; Margot-Roquier, C.; Webb, S. M.; Tebo, B. M.; Giammar, D. E.; Bargar, J. R.; Bernier-Latmani, R. Uranium speciation and stability after reductive immobilization in

DOI: 10.1021/acs.est.5b04281
Environ. Sci. Technol. 2016, 50, 1403−1411

aquifer sediments. *Geochim. Cosmochim. Acta* **2011**, *75* (21), 6497−6510.
(13) Wang, Y. H.; Frutschi, M.; Suvorova, E.; Phrommavanh, V.; Descostes, M.; Osman, A. A. A.; Geipel, G.; Bernier-Latmani, R. Mobile uranium(IV)-bearing colloids in a mining-impacted wetland. *Nat. Commun.* **2013**, *4*, 2942.
(14) Alessi, D. S.; Lezama-Pacheco, J. S.; Janot, N.; Suvorova, E. I.; Cerrato, J. M.; Giammar, D. E.; Davis, J. A.; Fox, P. M.; Williams, K. H.; Long, P. E.; Handley, K. M.; Bernier-Latmani, R.; Bargar, J. R. Speciation and reactivity of uranium products formed during in situ bioremediation in a shallow alluvial aquifer. *Environ. Sci. Technol.* **2014**, *48* (21), 12842−12850.
(15) Alessi, D. S.; Lezama-Pacheco, J. S.; Stubbs, J. E.; Janousch, M.; Bargar, J. R.; Persson, P.; Bernier-Latmani, R. The product of microbial uranium reduction includes multiple species with U(IV)-phosphate coordination. *Geochim. Cosmochim. Acta* **2014**, *131*, 115−127.
(16) Alessi, D. S.; Uster, B.; Veeramani, H.; Suvorova, E. I.; Lezama-Pacheco, J. S.; Stubbs, J. E.; Bargar, J. R.; Bernier-Latmani, R. Quantitative Separation of Monomeric U(IV) from UO2 in Products of U(VI) Reduction. *Environ. Sci. Technol.* **2012**, *46* (11), 6150−6157.
(17) Cerrato, J. M.; Ashner, M. N.; Alessi, D. S.; Lezama-Pacheco, J. S.; Bernier-Latmani, R.; Bargar, J. R.; Giammar, D. E. Relative reactivity of biogenic and chemogenic uraninite and biogenic noncrystalline U(IV). *Environ. Sci. Technol.* **2013**, *47* (17), 9756−9763.
(18) Abdelouas, A.; Lutze, W.; Nuttall, E. Chemical durability of uraninite precipitated on Navajo sandstone. *C. R. Acad. Sci., Ser. IIa: Sci. Terre Planetes* **1998**, *327* (2), 101−106.
(19) Moon, H. S.; Komlos, J.; Jaffé, P. R. Biogenic U(IV) oxidation by dissolved oxygen and nitrate in sediment after prolonged U(VI)/Fe(III)/SO_4^{2-} reduction. *J. Contam. Hydrol.* **2009**, *105* (1−2), 18−27.
(20) Hua, B.; Deng, B. L. Reductive immobilization of uranium(VI) by amorphous iron sulfide. *Environ. Sci. Technol.* **2008**, *42* (23), 8703−8708.
(21) Hyun, S. P.; Davis, J. A.; Sun, K.; Hayes, K. F. Uranium(VI) reduction by iron(II) monosulfide mackinawite. *Environ. Sci. Technol.* **2012**, *46* (6), 3369−3376.
(22) Bi, Y.; Hyun, S. P.; Kukkadapu, R. K.; Hayes, K. F. Oxidative dissolution of UO_2 in a simulated groundwater containing synthetic nanocrystalline mackinawite. *Geochim. Cosmochim. Acta* **2013**, *102* (0), 175−190.
(23) Bi, Y.; Hayes, K. F. Nano-FeS inhibits UO_2 reoxidation under varied oxic conditions. *Environ. Sci. Technol.* **2013**, *48* (1), 632−640.
(24) Suzuki, Y.; Kelly, S. D.; Kemner, K. M.; Banfield, J. F. Direct microbial reduction and subsequent preservation of uranium in natural near-surface sediment. *Appl. Environ. Microbiol.* **2005**, *71* (4), 1790−1797.
(25) Bi, Y.; Hayes, K. F. Surface passivation limited UO_2 oxidative dissolution in the presence of FeS. *Environ. Sci. Technol.* **2014**, *48* (22), 13402−13411.
(26) Ginder-Vogel, M.; Stewart, B.; Fendorf, S. Kinetic and mechanistic constraints on the oxidation of biogenic uraninite by ferrihydrite. *Environ. Sci. Technol.* **2010**, *44* (1), 163−169.
(27) Sani, R. K.; Peyton, B. M.; Dohnalkova, A.; Amonette, J. E. Reoxidation of reduced uranium with iron(III) (hydr)oxides under sulfate-reducing conditions. *Environ. Sci. Technol.* **2005**, *39* (7), 2059−2066.
(28) Jeong, H. Y.; Lee, J. H.; Hayes, K. F. Characterization of synthetic nanocrystalline mackinawite: Crystal structure, particle size, and specific surface area. *Geochim. Cosmochim. Acta* **2008**, *72* (2), 493−505.
(29) Jeong, H. Y.; Han, Y. S.; Park, S. W.; Hayes, K. F. Aerobic oxidation of mackinawite (FeS) and its environmental implication for arsenic mobilization. *Geochim. Cosmochim. Acta* **2010**, *74* (11), 3182−3198.
(30) Schwertmann, U.; Cornell, R. M. *Iron Oxides in the Laboratory: Preparation and Characterization*, 2nd ed.; Wiley-VCH: Weinheim ; New York, 2000; pp 1−188.
(31) Pablo, J. D.; Casas, I.; Gimenez, J.; Molera, M.; Rovira, M.; Duro, L.; Bruno, J. The oxidative dissolution mechanism of uranium dioxide. I. The effect of temperature in hydrogen carbonate medium. *Geochim. Cosmochim. Acta* **1999**, *63* (19−20), 3097−3103.
(32) Wolthers, M.; Charlet, L.; Van der Linde, P. R.; Rickard, D.; Van der Weijden, C. H. Surface chemistry of disordered mackinawite (FeS). *Geochim. Cosmochim. Acta* **2005**, *69* (14), 3469−3481.
(33) Mikhlin, Y. Disordered surface layers of metal sulfides and their reactivity. *Glass Phys. Chem.* **2007**, *33* (4), 402−410.
(34) Mikhlin, Y.; Varnek, V.; Asanov, I.; Tomashevich, Y.; Okotrub, A.; Livshits, A.; Selyutin, G.; Pashkov, G. Reactivity of pyrrhotite (Fe9S10) surfaces: Spectroscopic studies. *Phys. Chem. Chem. Phys.* **2000**, *2* (19), 4393−4398.
(35) Ginder-Vogel, M.; Fendorf, S. Chapter 11: Biogeochemical Uranium Redox Transformations: Potential Oxidants of Uraninite. In *Developments in Earth and Environmental Sciences*; Mark, O. B.; Douglas, B. K., Eds. Elsevier: Amsterdam, Netherlands, 2007; Vol. *7*, pp 293−319.
(36) Ilton, E. S.; Bagus, P. S. XPS determination of uranium oxidation states. *Surf. Interface Anal.* **2011**, *43* (13), 1549−1560.
(37) Mullet, M.; Boursiquot, S.; Abdelmoula, M.; Genin, J. M.; Ehrhardt, J. J. Surface chemistry and structural properties of mackinawite prepared by reaction of sulfide ions with metallic iron. *Geochim. Cosmochim. Acta* **2002**, *66* (5), 829−836.
(38) Grosvenor, A. P.; Kobe, B. A.; Biesinger, M. C.; McIntyre, N. S. Investigation of multiplet splitting of Fe 2p XPS spectra and bonding in iron compounds. *Surf. Interface Anal.* **2004**, *36* (12), 1564−1574.
(39) Wehrli, B.; Sulzberger, B.; Stumm, W. Redox processes catalyzed by hydrous oxide surfaces. *Chem. Geol.* **1989**, *78* (3−4), 167−179.
(40) Chirita, P. Iron monosulfide (FeS) oxidation by dissolved oxygen: characteristics of the product layer. *Surf. Interface Anal.* **2009**, *41* (5), 405−411.
(41) Stumm, W.; Lee, G. F. Oxygenation of Ferrous Iron. *Ind. Eng. Chem.* **1961**, *53* (2), 143−146.
(42) Veeramani, H.; Scheinost, A. C.; Monsegue, N.; Qafoku, N. P.; Kukkadapu, R.; Newville, M.; Lanzirotti, A.; Pruden, A.; Murayama, M.; Hochella, M. F. Abiotic reductive immobilization of U(VI) by biogenic mackinawite. *Environ. Sci. Technol.* **2013**, *47* (5), 2361−2369.
(43) Ulrich, K. U.; Ilton, E. S.; Veeramani, H.; Sharp, J. O.; Bernier-Latmani, R.; Schofield, E. J.; Bargar, J. R.; Giammar, D. E. Comparative dissolution kinetics of biogenic and chemogenic uraninite under oxidizing conditions in the presence of carbonate. *Geochim. Cosmochim. Acta* **2009**, *73* (20), 6065−6083.

DOI: 10.1021/acs.est.5b04281
Environ. Sci. Technol. 2016, 50, 1403−1411